

ANALYSIS OF A PRESSED COMPOSITE AUTOMOTIVE TAILGATE USING ANSA & μETA

Andy Ngai, Mark Arnold
Penso, UK

KEYWORDS – Composites, Design Optimization, Failure, Finite Element Analysis, Laminate

ABSTRACT – Composite materials utilised within the automotive industry have increased in recent times, due to the demand to reduce weight and vehicle CO₂ emissions. Penso were commissioned by a European automotive OEM to design and manufacture a prototype continuous fibre reinforced composite tailgate. The main objective for the composite design was to minimise mass, whilst meeting all strength and stiffness targets of the production SMC tailgate. Three main parts of the tailgate considered for light weighting were the tailgate inner panel, tailgate outer panel and spoiler mechanism carrier. The laminate tool function within the pre-processor ANSA was utilised for ease of building, handling and modifying the composite model. A laminate design was developed using non-linear static FE analysis. Results were plotted using the post-processor μETA, with the Tsai-Wu failure criterion and a user defined inter-laminar failure criterion used as design metrics. The laminate design was then assessed by Penso's composite manufacturing team to develop overlap joint locations and preliminary ply shapes appropriate for processing utilising Penso's pressed composite technology. Ply shapes and draped material directions were updated in the FE model for further refinement and prediction of finalised mass/performance. The final composite design resulted in a combined mass save of over 65% whilst having comparable structural performance to the SMC production design.

TECHNICAL PAPER -

1. INTRODUCTION

Penso were commissioned to design and manufacture a continuous fibre reinforced composite tailgate. This would be a lightweight alternative to the current production tailgate which is manufactured from Sheet Moulding Compound (SMC), a discontinuous glass-fibre reinforced polymer material.

2. TAILGATE DESIGN

The production tailgate comprises of a bonded sub-assembly of the inner and outer SMC panels, with a steel spoiler mechanism carrier bolted to the outer panel, as illustrated in Figure 1. Metallic reinforcing mounting plates for the hinges, gas struts and latch are bonded to the inside of the inner panel, with the rear screen glass bonded to the outer panel. The individual masses of the three main panels are 5.7 kg, 3.2 kg and 1.1 kg for the tailgate SMC inner panel, tailgate SMC outer panel and the steel spoiler mechanism carrier respectively, providing a total mass for the three panels of 10.05kg.

The three main parts of the tailgate that were considered for light weighting; were the tailgate inner panel, tailgate outer panel and the spoiler mechanism carrier. The requirements of the new composite design had to meet all existing strength and stiffness performance targets, whilst also preserving existing A-surface geometry and hardware. The load cases used to assess the structural performance targets against of the tailgate were torsion, cantilevered bending, latch load and margin & flushness.

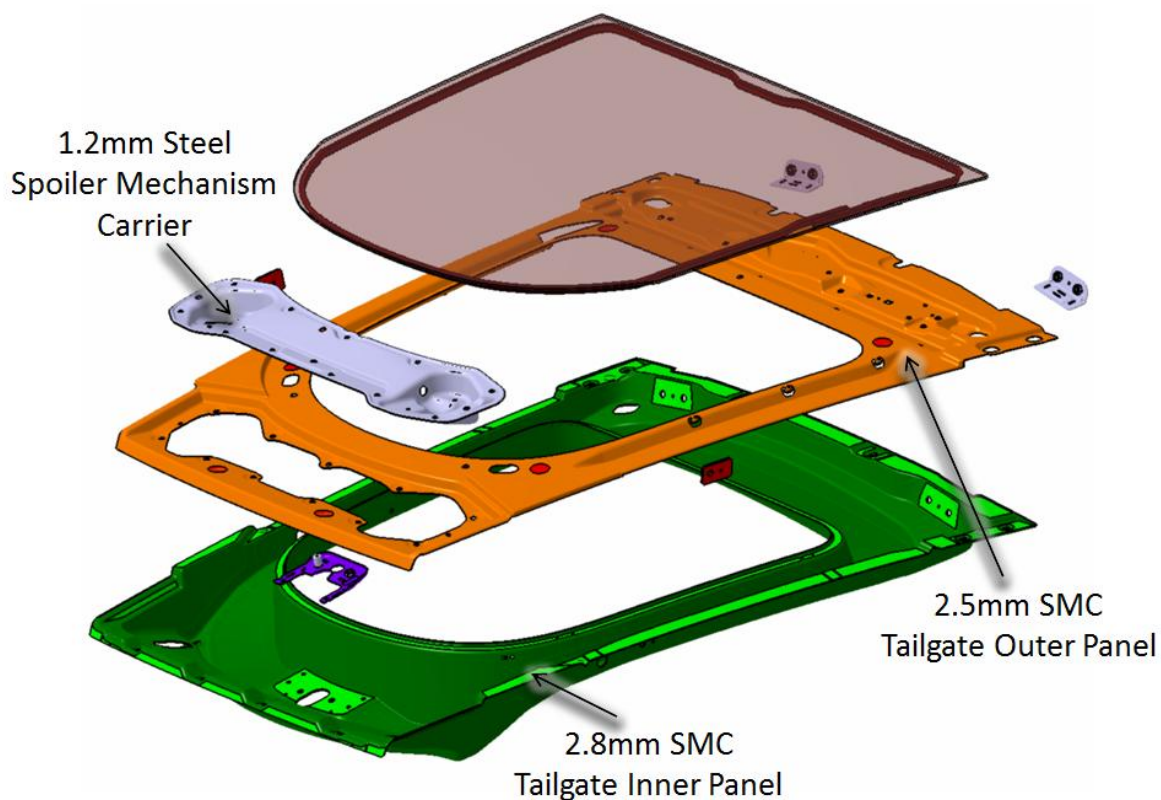


Figure 1. Tailgate parts considered for light weighting.

The composite parts comprised a continuous fibre reinforced polymer material, using pre-impregnated (prepreg) epoxy resin carbon fibre reinforcement. The composite parts were laminated from a single prepreg composite sheet material. The carbon fibre material used was the Cytec 2020-40%-6KHS-2x2T-400, which is a 2x2 Twill woven fabric, supplied by Cytec Industries. Static coupon tests were performed for this prepreg to obtain mechanical properties in longitudinal (warp) and lateral (weft) fibre directions. Validation of these material models were carried out through simulation of coupon testing performed according to various ASTM test methods (Arnold et al, 2014).

Penso's pressed composite technology will be utilised to manufacture the composite parts of the prototype tailgate, this is a process in which the prepreg composite material is placed into an open matched metal mould cavity. The tool is then closed under pressure to encapsulate the fibre and resin compound within the mould cavity. Heat and pressure are maintained until the composite material has cured.

3. LAMINATE OPTIMISATION

3.1. Finite element model

ANSA pre-processing software was used to import CAD geometry and converted into a surface suitable for shell meshing. The mesh was created on the A-surface which corresponded to the preform tool surface so that the laminate plies stacked from A to B surface. Each panel was meshed with first order conventional S4 and S3R shell elements, having mesh size of approximately 5mm. These elements were utilised for their accurate solutions for in-plane bending problems.

The laminates tool within ANSA was utilised for the ease of building, handling and modifying of all the layers of the composite model, which exploits a special ANSA laminate property. This ANSA laminate property simplifies the number of layers the user has to manage during pre and post-processing e.g. the inner panel comprised 1 laminate having 49 layers compared to the 244 composite shell section properties having a total of 1351 plies when written out to the Abaqus/Standard FE solver. The 244 composite shell section properties

that exist, when ANSA comments are not read in, are shown in Figure 2. With fewer plies to manage there is less room for error during pre and post-processing. As draping simulation was not performed during the development of the prototype tailgate, the material orientation was defined within ANSA by projecting a vector of the fore/aft direction onto every element.

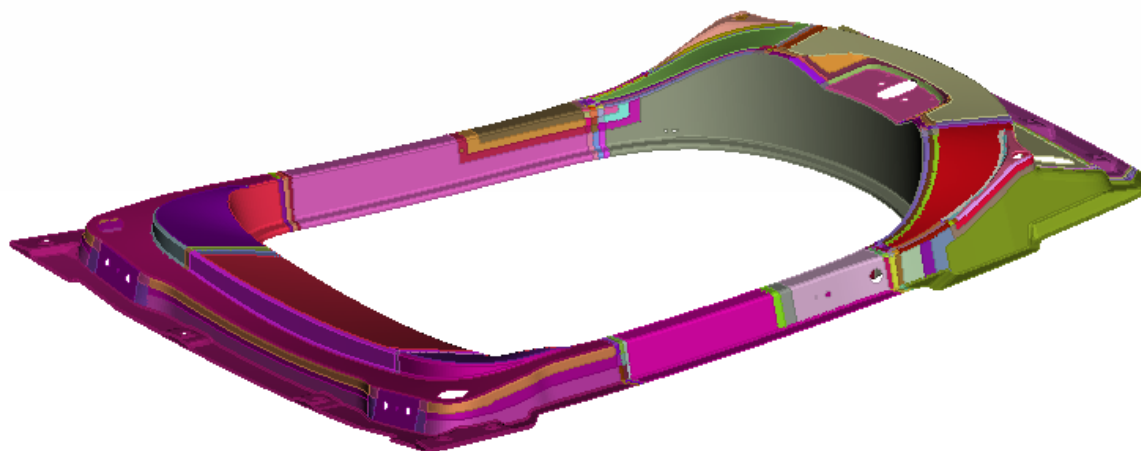


Figure 2. Composite shell properties on the inner panel.

Abaqus/Standard 6.12-2 was used for the non-linear static finite element analysis of the tailgate. The carbon fibre panels were modelled with laminate properties defined using *SHELL SECTION, COMPOSITE. For the orthotropic carbon fibre skins an *ELASTIC, TYPE=LAMINA material card was used with *FAIL STRESS to define the strength terms. The modulus of elasticity for warp and weft directions were both set to the minimum of these two values obtained from tensile test data, however it was noted that these values differed from those derived by compression tests. The tensile/compressive strengths in warp and weft directions were both reduced to the open hole tensile/compressive strength to incorporate hole and defect tolerance, a method proposed by Niu (1992). The resulting knock down factors were 0.75 for tensile strength and 0.45 for the compressive strength.

To complete the tailgate model, the adhesive was modelled using solid elements, referencing isotropic elastic materials properties, connected to neighbouring panels using the distributing coupling constraints. The metallic mounting plates were modelled as shell elements referencing non-linear elastic-plastic material properties, whilst the rear glass was modelled with shell elements referencing isotropic elastic material properties.

3.2. Deriving an optimised laminate design

An optimised layout for the composite panels, which disregarded joints between all-over plies, was derived to comply with the structural performance targets, whilst also minimising mass. The optimised layout was derived through the use of analysis tools within the μ ETA post-processor. The μ ETA post-processor was used to extract results for the non-linear static analysis of the composite tailgate for comparison with structural performance targets. The CompositePost Toolbar within μ ETA was used to process the composite materials within the analysis. The toolbar offers a set of integrated specialized functionalities which is within a single user interface for ease of use. Useful functionalities available to the user are the possibility to Identify layer id of max failure, Max/min of all layers, Identify critical direction, 2d DNA plot for failure criterion results for multiple elements and a 2D plot of failure criterion and stress tensor per layer can also be plotted.

Within the 2d plot window there are three plots which assist with the analysis of the composite material parts showing detailed information regarding each element. In Figure 3, detailed information regarding the element which had the highest failure criterion is shown for an earlier preliminarily layout; the layout at this element is [45/0/0/45].

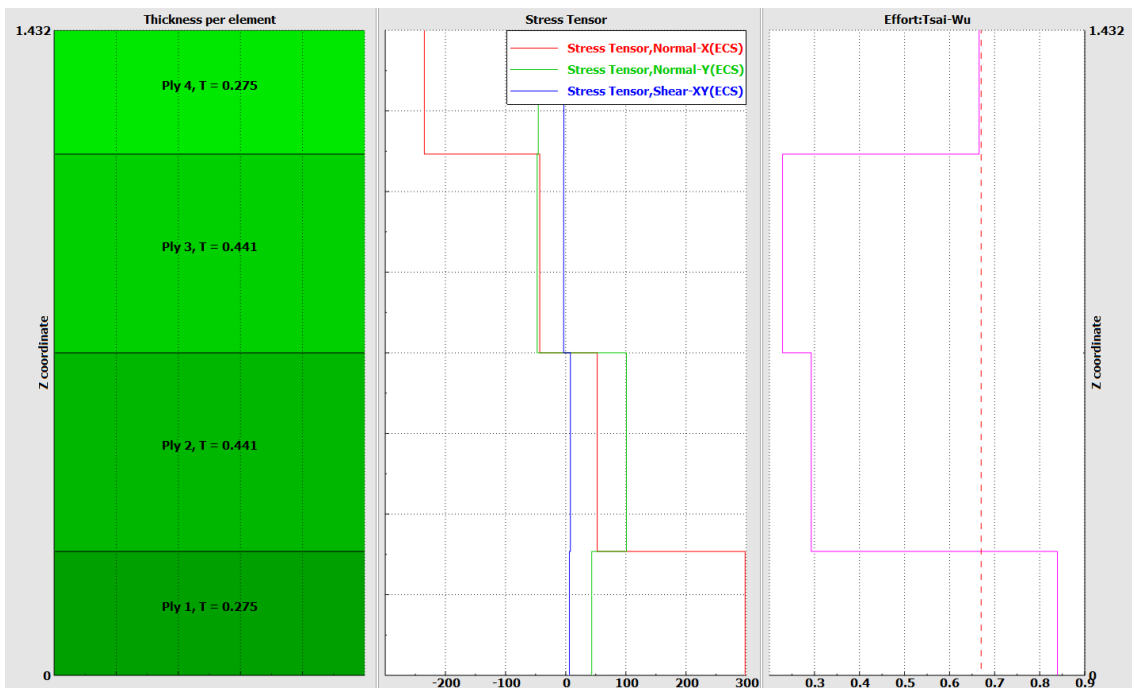


Figure 3. 2D plot vs thickness of preliminary layout.

The left part of the plot illustrates the distribution of the layers along the total thickness of the element. The middle part of the plot contains three curves corresponding to the stress tensor components results along the thickness. The right part of the plot contains a curve corresponding to the failure criterion result along the thickness, where failure criterion is a composite design metric used to determine if ply failure will occur within the laminate. This failure criterion plot is the most useful plot to understand and reduce the failure criterion value. In Figure 3 the plies which exceed or are close to the critical value of 0.67 are plies 1 and 4 with a value of 0.84 and 0.66 respectively. To reduce this value, the material of the 45° plies, 1 and 4, were changed from the 240gsm material to the 400gsm, which increased the thickness of the ply from 0.275mm to 0.441mm. The failure criterion for ply 2 and 3 were seen to be relatively low with a value of 0.29 and 0.23 respectively, therefore an opportunity to remove one of these 0° plies was seen possible to reduce mass without compromising the strength excessively.

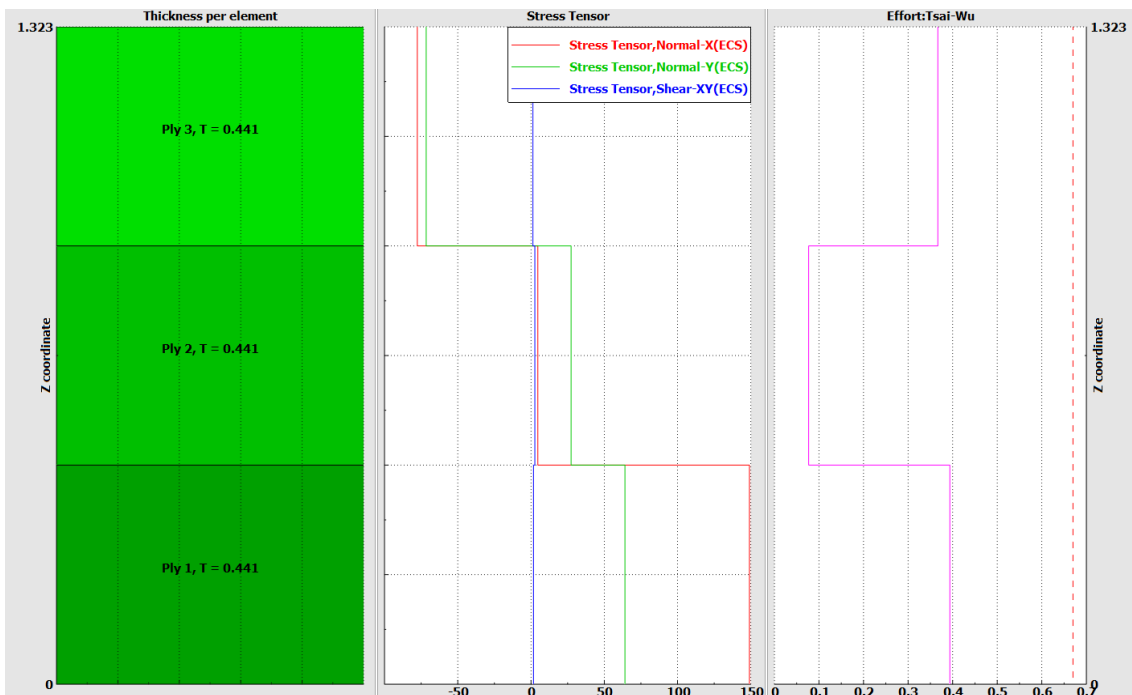


Figure 4. 2D plot vs thickness of optimised layout.

Figure 4 shows a 2d plot vs thickness for the same element as was shown in Figure 3, incorporating the change in thickness of the 45° plies to 0.441mm thick and removing a single 0° ply giving a layup of [45/0/45]. The failure criterion value has now decreased to 0.39, 0.08 and 0.37 for ply 1, 2 and 3 respectively, which are all below the critical value of 0.67. This method shows that the element with the highest failure criterion value complies with the critical value, therefore the composite parts complies with the structural performance target and the layup was deemed optimised.

3.3. Optimised laminate design

To reduce the possibility of distortion during the manufacturing process the composite panels were constrained to have a minimum thickness of two all-over plies and a symmetric balanced laminate.

The optimised laminate for the outer panel consists of two all-over plies at 45° relative to the material orientation axes, with an extra local reinforcement ply at 0° positioned where the spoiler mechanism carrier is attached. The optimised laminate for the inner panel comprises three all-over plies at 45°, 0° and 45°, with three extra local reinforcement plies at 45°, 0° and 45° enclosed within the main laminate. These reinforcement plies are positioned at the four corners of the panel to improve global stiffness, and also locally at the latch, hinge and gas strut mounting region to improve the strength within these areas. Figure 5 shows a thickness plot of the optimised layup for the inner and outer tailgate panels. The laminate for the spoiler mechanism carrier simply consists of three all-over plies at 0°, 45° and 0°.

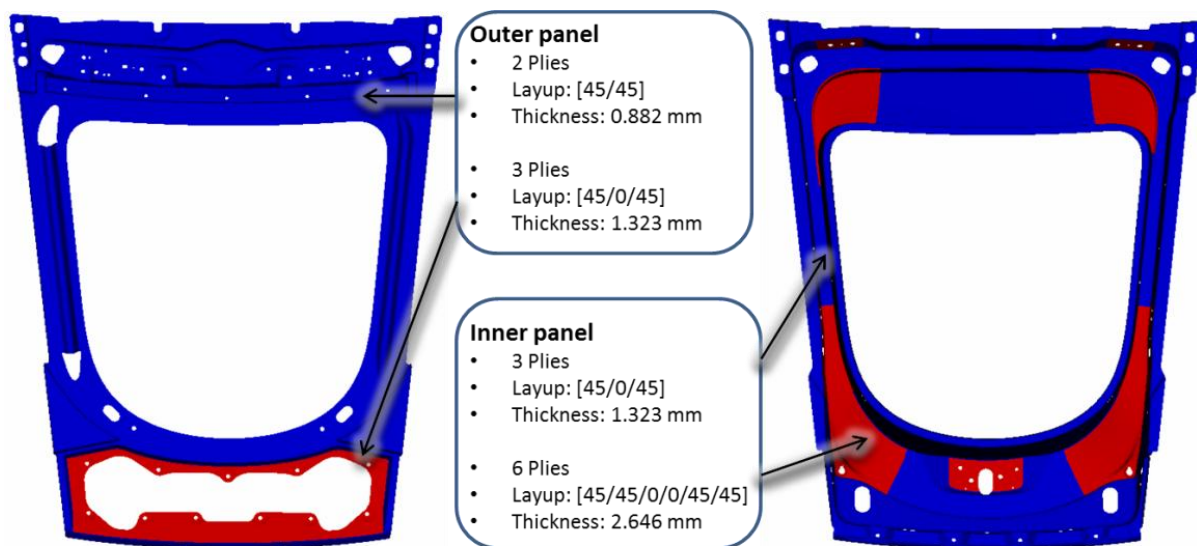


Figure 5. Optimised laminate design for tailgate inner and outer panel.

3.4. Finite element results for optimised laminate design

For post processing, Tsai-Wu Failure Measure and a user defined Inter-Laminar Failure Criterion were used as composite design metrics to determine whether ply failure or delamination would occur. μ ETA post-processor was utilised to plot Tsai-Wu Failure Measure results. The Tsai-Wu Failure Measure values are plotted at the in-plane integration points at the mid-section point per ply. The in-plane integration point results were used since these are the locations where results are typically more accurate (Cook et al, 1989). It was also believed that by extrapolating the results at the integration points to the corners may introduce additional uncertainties in failure measures. For the user-defined Inter-Laminar Failure Index, output values were taken at surface section points of each ply. Nodal displacements were taken at certain pre-defined nodes, depending on the load case, to ensure compliance with stiffness targets.

3.4.1. Failure index

For the post processing of the laminate, the Tsai-Wu Failure Measure was used. The Tsai-Wu Failure Measure is used with composite materials under loading. A value greater than 1

indicates failure. The Tsai-Wu Failure Measure is proportional to applied load, unlike other available failure criterion's such as Failure index and Strength Ratio, with the maximum value indicate high stress regions, this makes it more intuitive for the user to post process results.

A safety factor of 1.5 was considered for strength assessment to account for load variability, (Niu, 1992). Rather than incorporate this safety factor into the material strength terms, this was instead incorporated during post processing by ensuring the maximum Tsai-Wu Failure Measure value was <0.67. This was also believed to provide some robustness against variation in material allowables and uncertainty in FEA methods.

Figure 6 shows a Tsai-Wu Failure Measure plot for the torsion load case. For this load case, a vertical Z-direction load of 267N is applied at the right hand bump stop, while the left hand bump stop is constrained in z-direction and the hinges constrained in all DOF. The max Tsai-Wu Failure Measure is 0.36, indicating ply failure will not occur.

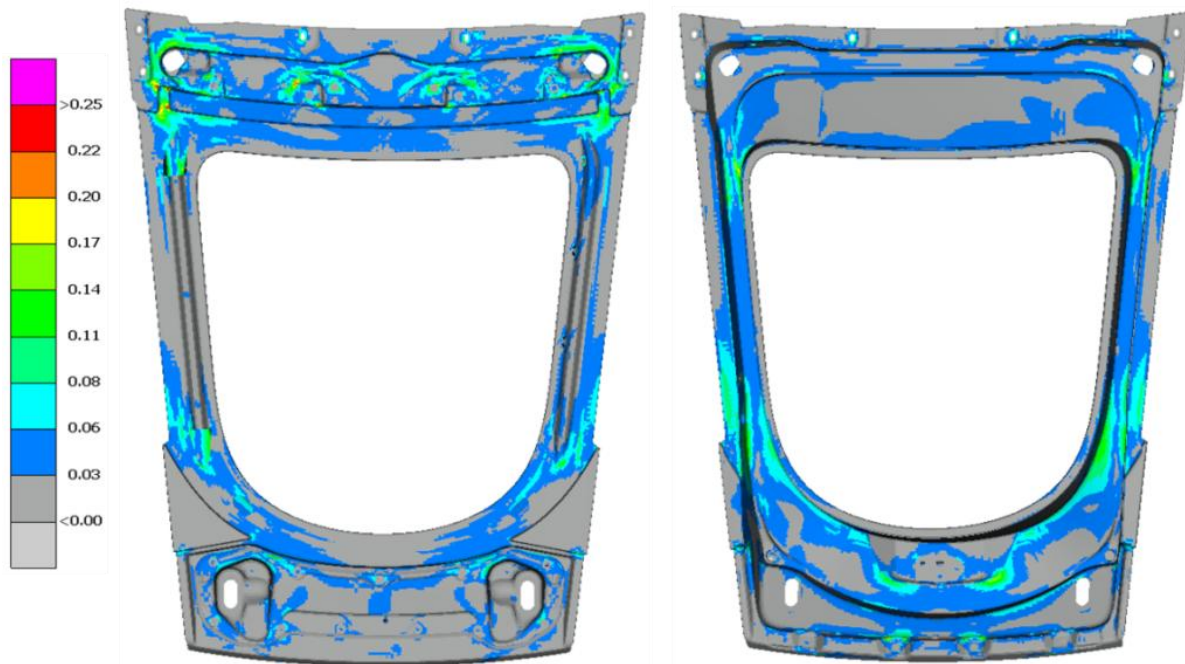


Figure 6. Tsai-Wu failure measure plot for torsion load case.

3.4.2. Interlaminar shear

Interlaminar shear stress, an indication if delamination would occur, is analysed through the use of the output variable transverse shear stress. Transverse shear stress (TSHR) was requested in Abaqus/Standard to output results for transverse shear stress in the 13-component, τ_{13} , and transverse shear stress in the 23-component, τ_{23} , for each ply boundary for every element. The resultant transverse shear stress was calculated from τ_{13} and τ_{23} and this can then be used in a user defined equation shown in Equation 1 to calculate the Inter-Laminar Failure Index (Bednarczyk et al, 2008). The allowable Inter-laminar shear strength Fsu_{13} and Fsu_{23} was assumed to be the same for the woven fabric.

$$Inter - Laminar Failure Index = \sqrt{\left(\frac{\tau_{13}}{Fsu_{13}}\right)^2 + \left(\frac{\tau_{23}}{Fsu_{23}}\right)^2} \quad (1)$$

Figure 7 shows a resultant transverse shear stress plot for the torsion load case. The max resultant transverse shear stress was found to be 9.79 MPa, which gave an Inter-Laminar Failure Index of 0.20, indicating delamination would not occur.

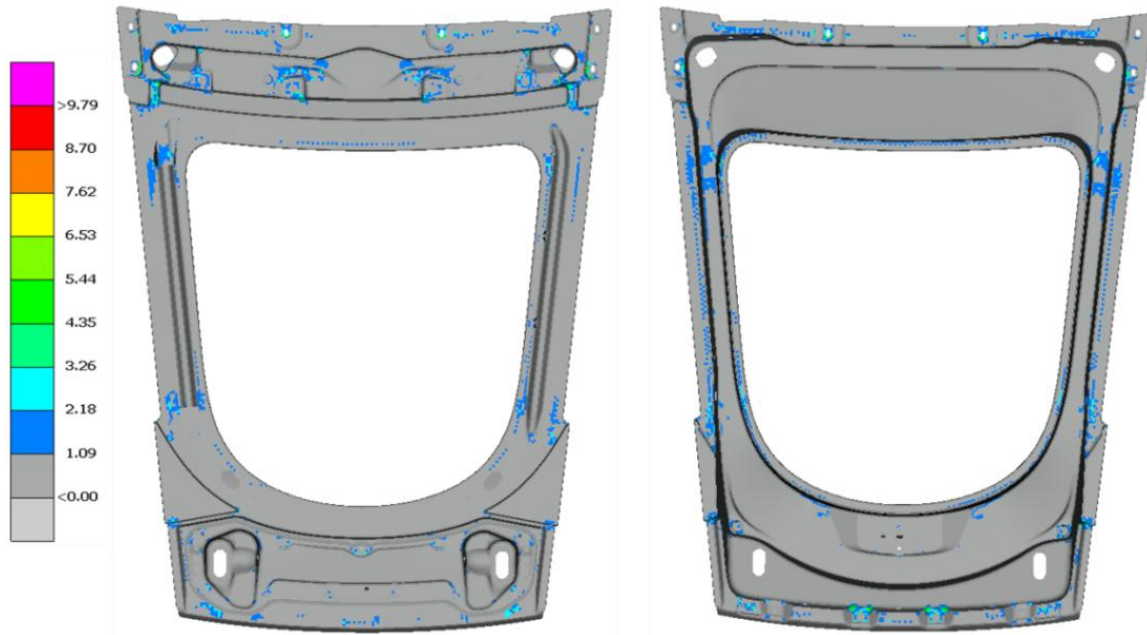


Figure 7. Resultant transverse shear stress plot for torsion load case.

3.4.3. Adhesive

Major Principal Stress and Max Shear Stress along with the corresponding allowable stresses for tensile and shear, were used to calculate a failure index to determine if tensile and shear failure would occur within the adhesive. This method, when combined with the linear elastic material model, gives a conservative result. The stresses found within the analysis were very low, therefore a more detailed assessment for the adhesive was considered unnecessary.

3.4.4. Displacement

Figure 8 shows a displacement plot for the torsion load case. By using the z-deflection at the unconstrained right hand bump stop and the distance between the two bump stops, the twist angle can be derived using trigonometry. The derived twist angle was 1.63 degrees.

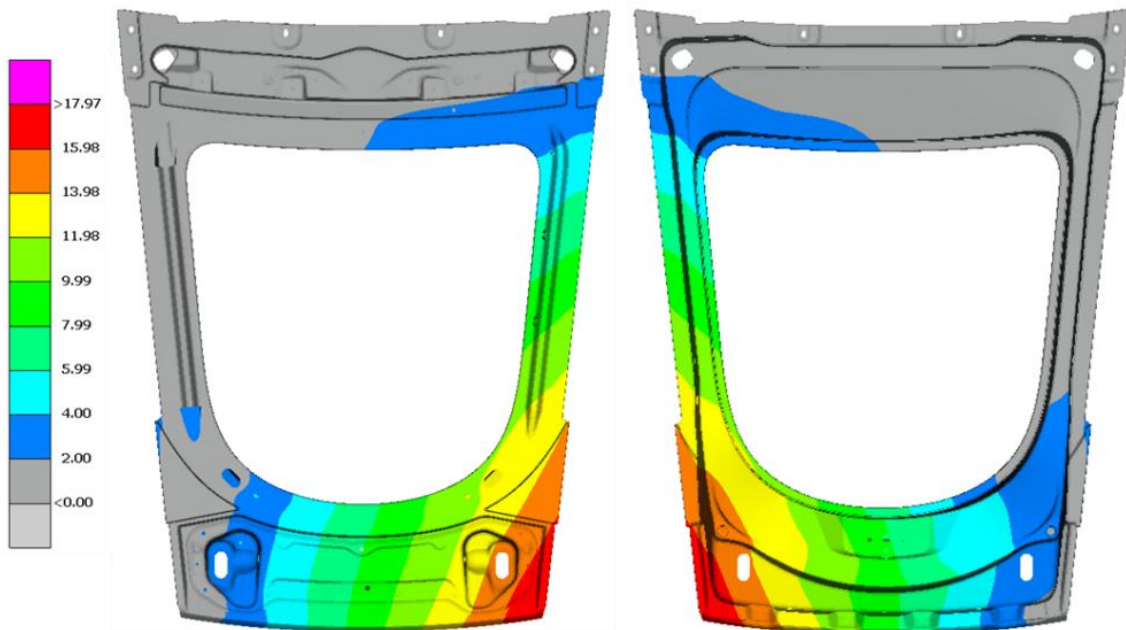


Figure 8. Displacement plot for torsion load case.

3.4.5. Results summary

Table 1 shows the results of the optimised composite tailgate for the torsion load case, discussed in sections 3.3.1, 3.3.2 and 3.3.4, along with the results for the other three tailgate load cases. From Table 1 it can be seen that the stiffness results comply with the targets set, apart from the torsion load case where the twist angle slightly surpasses the 1.6 degree target by 2%. However, this value was considered to be acceptable in the expectation that the additional overlaps into the final tailgate model will improve the torsional performance. The strength results also comply with Penso's target of <0.67 for Tsai-Wu Failure Measure and Inter-laminar shear failure index. It was found that the composite tailgate laminate design was driven mainly by the stiffness requirements, particularly for the torsion load case, which is an important reason the tailgate outer and inner panel laminates are biased to plies oriented at 45 degree.

Load case	Deflection Target	Deflection Result	Max Tsai-Wu Failure Measure	Max Interlaminar Shear FI
Latch Load	< 1 mm	0.11 mm	0.14	0.05
Torsion	< 1.6 degrees	1.63 degrees	0.36	0.20
Margin & Flushness	< 2 mm	1.29 mm	0.53	0.28
Cantilevered Bending	< 0.85 mm	0.02 mm	0.24	0.12

Table 1. Optimised tailgate load case results.

4. DESIGN FOR MANUFACTURE

The optimised laminate design was evaluated by Penso's composite manufacturing team to develop the preliminary ply shapes and overlap joint locations. That are suitable for manual draping and applicable to Penso's pressed composite technology. A preform tool was manufactured to the preliminary A-surface geometry and used for layup trials. Due to the complex geometry of the tailgate inner and tailgate outer panels, each of the all-over plies was subsequently divided into approximately twelve separate overlapped pieces to enable draping of the prepreg. The overlap distance between any two plies was typically 10mm, to ensure a smooth A-Surface the step in laminate thickness was located on the B-Surface. Attention to the detailed joint architecture was essential as the use of butt joints alone does not allow the transfer of loads from one ply to another, unlike overlap joints. Therefore, overlap joints were considered to be more desirable. Figure 9 shows an example of a staggered overlap joint used. The lower ply of an overlap joint is butt jointed to the upper ply of the previous overlap joint. This method of staggering the overlaps reduces the thickness variation across the joint, which makes things easier during the manufacturing stages.



Figure 9. Staggered overlap joint between three plies.

Once the ply layup and overlap locations had been developed for manufacture, the ply boundaries documented by the laminator in their draped configuration were passed to Penso's analysis team along with detailed information concerning fibre distortion. These ply boundaries, overlap locations and material directions were then incorporated into the FE model for prediction of refined mass/performance data and the generation of layup manuals. Material directions gained from layup trials were compared to those in the analysis model and modifications were made where large inconsistencies existed between the two sets of data. As the parts were to be manufactured using layup books generated directly from the FE models the ply shapes needed to be accurately defined.

Figures 10 and 11 show thickness plots for the updated FE model of the tailgate outer and inner panels respectively, incorporating the ply boundaries and overlap locations determined by the manufacturing team.

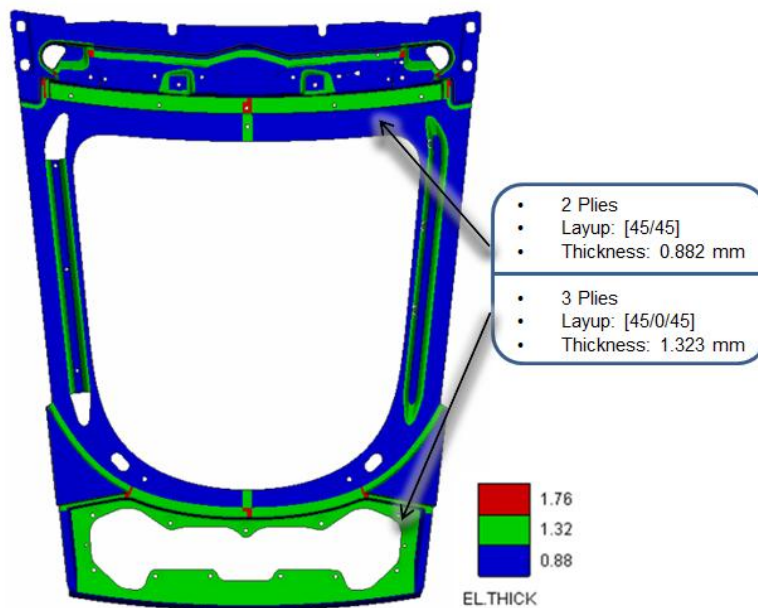


Figure 10. Thickness plot of final tailgate outer panel including overlap joints.

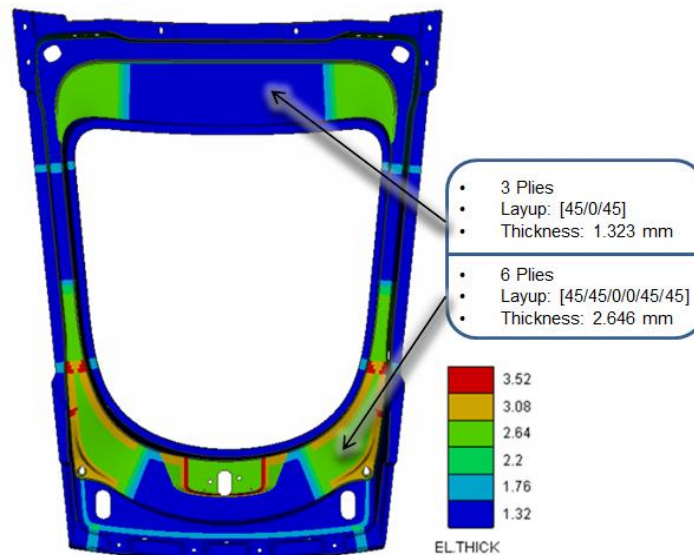


Figure 11. Thickness plot of final tailgate inner panel including overlap joints.

The load cases for the updated tailgate model which included overlap joints were rerun. It was observed that due to the thicker regions added to represent the overlaps the performance of the structure increased marginally, as shown in Table 2. As classical laminate shell theory is being used to represent the laminate, the performance is expected to increase due to the increase in thickness at these overlap regions. However this does not accurately represent the joint, as the reduction in strength due to the discontinuity of the plies is not considered.

Load case	Deflection Target	Deflection Result	Max Tsai-Wu Failure Measure	Max Interlaminar Shear FI
Latch Load	< 1 mm	0.10 mm	0.12	0.04
Torsion	< 1.6 degrees	1.30 degrees	0.25	0.14
Margin & Flushness	< 2 mm	1.83 mm	0.48	0.20
Cantilevered Bending	< 0.85 mm	0.02 mm	0.21	0.10

Table 2. Final tailgate load case results.

By incorporating the overlaps within the model, it is possible to determine a more accurate mass prediction for the composite parts. The mass increase due to the overlaps was approximately 10% per panel. Table 3 shows a mass breakdown for the three composite panels, it can be seen that the mass of these panels were 2.3kg, 0.9kg and 0.2kg for the tailgate inner, tailgate outer and spoiler mechanism carrier respectively. This equates to a total mass of 3.4kg, which is a 6.6kg or 66% mass reduction compared to the current production tailgate.

	Production SMC Mass	Prototype CFRP Mass
Tailgate Inner	5.7 kg	2.3 kg
Tailgate Outer	3.2 kg	0.9 kg
Spoiler Mechanism Carrier	1.1 kg	0.2 kg
Total	10.0 kg	3.4 kg

Table 3. Final tailgate mass.

By modelling the layup from the A-Surface and taking into account the ply shapes and ply thickness, the B-Surface could be generated for the composite parts of the tailgate. The A and B-surfaces of the composite parts can then be used to create tool geometry for manufacturing.

5. CONCLUSION

The main objective of this project was to demonstrate that by using a composite material on the production tailgate weight reduction could be achieved, whilst also achieving comparable results to the targets/baseline. Results from the FE analysis indicate that all strength and stiffness targets were achieved for the composite tailgate, whilst having equivalent or improved structural performance to that of the current production tailgate. Total mass of the prototype carbon fibre tailgate panels was 3.4kg, providing a mass saving of 6.6kg or 66%, compared to the corresponding SMC/steel panels. However, the overall mass saving of the whole tailgate assembly was greater than 66%. This is due to the removal of extra components such as the anti-pinch strips, addition of a new lightweight rear screen glass and also incorporating the interior trim into the carbon fibre parts.

Further improvements which could have been made to improve the design are by redesigning the geometry of the tailgate so that it is specific for carbon fibre use. The section depth could be reduced, rather than use carry over geometry designed for lower strength and stiffness materials. This would improve the draping of the material and also reduce the complexity during the pre-forming phase, which will improve the optical quality of the finished composite parts. Location of the ply overlap joints were positioned to optimise the global stiffness, whereas preferably they should be located in less visible areas to provide the best aesthetics. Metallic mounting plates, which have been carried over from the original production design, such as at the hinge, latch and gas strut mounting areas, could be replaced by metallic inserts to reduce the assembly part count and total mass.

Further work has been carried out since, to improve the process of Penso's pressed composite technology. Various draping simulation softwares have been assessed to determine how accurately they are able to predict ply orientation/distortion due to draping over complex geometry. The accurate material orientations would ensure the analysis models accurately reflect the design intent data and would evaluate ply producibility during the design phase to avoid any potential difficulties which may occur during manufacturing. Robustness studies have been carried out to produce a practical method for quantifying the variability of continuous fibre-reinforced composite structures to uncertainty in ply orientation. Continuous progress is being carried out with Penso's laminators to develop the layup of the tailgate composite panels to reduce laminating time, yet still achieve equivalent structure performance.

6. ACKNOWLEDGEMENTS

This project was co-funded by Innovate UK as part of the IDP7 Low Carbon Vehicles programme, in which Penso were a lead manufacturing partner.

7. REFERENCES

- (1) Arnold, M., Kilby, C. & Ngai, A. (2014). Validation of Laminated Composite Shell Elements and Material Models within Various FEA Solvers. Proceedings of NAFEMS UK 2014 Conference, Oxford, June 2014.
 - (2) Bednarczyk, B.A., Aboudi, J., Yarrington, P.W., Collier, C.S., (2008). Simplified Shear Solution for Determination of the Shear Stress Distribution in a Composite Panel from the Applied Shear Resultant. Proceedings of 49th AIAA/ASME/ASCE/AHS/ASC Structures, Structural Dynamics, and Materials Conference, Schaumburg, IL, April 2008.
 - (3) Cook R.D., Malkus D.S. & Plesha M.E., (1989). Concepts and Applications of Finite Element Analysis, Third Edition. Chichester: John Wiley & Sons.
 - (4) Niu, M. (1992). Composite Airframe Structures: Hong Kong Conmilit Press Ltd.
 - (5) Abaqus Users Manual, Version 6.12-1, Dassault Systèmes Simulia Corp., Providence, RI.
-